Physiology and Pharmacology 30 (2026) 199-209
Experimental Research Article

Effect of umbilical cord mesenchymal stem cells and *Cichorium intybus* L. root extract on sciatic nerve regeneration

Amirhosein Fazlali[1], Nasim Hayati-Roodbari[1*], Gholam Reza Kaka[2], Kazem Parivar[1], Mohammad Kamalinejad[3]

1. Department of Biology, SR.C., Islamic Azad University, Tehran, Iran
2. Baqiyatallah University of Medical Sciences, Tehran, Iran
3. Pharmacognosy Department, Faculty of Pharmacy, Shahid Beheshti University of Medical Sciences, Tehran, Iran

ABSTRACT

Introduction: Peripheral nerves have limited self-restoration ability, but targeted nerve regeneration can be increased by growth factors, extracellular matrix addition, and stem cells. This study investigated the effects of umbilical cord stroma stem cells grown on nanopoly (lactic-co-glycolic acid) (PLGA) scaffolds of *Cichorium intybus* L. to repair the severed sciatic nerve of male Wistar rats.

Methods: Isolation of umbilical cord stroma stem cells and primary culture were done. After extracting from *Cichorium intybus* L., a PLGA scaffold was fabricated. Forty-five adult male Wistar rats (230-260 g) were divided into nine groups (healthy control, sciatic nerve injury, sciatic nerve injury treated with umbilical cord cells, sciatic nerve injury treated with *Cichorium intybus* L., sciatic nerve injury treated with *Cichorium intybus* L.+umbilical cord cells, sciatic nerve injury treated with *Cichorium intybus* L.+PLGA scaffold, nerve injury treated with PLGA scaffold, nerve injury treated with PLGA scaffold+umbilical cord cells, and nerve injury treated with *Cichorium intybus* L.+PLGA scaffold+umbilical cord cells). After eight weeks of treatment, the evaluation of sciatic nerve damage repair included electrophysiological and sciatic functional indexes, tissue sampling and immunocytochemistry, and histopathological examination.

Results: In the group treated with *Cichorium intybus* L.+PLGA scaffold+umbilical cord cells, sciatic nerve repair was observed with an increase in nerve conduction velocity (m/s), amplitude muscle action potential (mV), number of vessels and fiber, most significant area of vessels, myelin, axon, and fiber (1000 μm^2), and a decrease in statistic functional index (0 to -50) ($p<0.0001$).

Conclusion: It can be concluded that the transplantation of umbilical cord cells leads to the repair of the severed sciatic nerve. Also, the PLGA acts as a scaffolding to place cord stem cells and *Cichorium intybus* L.extract by reducing inflammation caused by surgery, and helps to recover faster.

Keywords:
Cichorium intybus L.
Mesenchymal stem cells
Poly lactic-co-glycolic acid scaffold
Sciatic nerve
Neural repair

* Corresponding author: Nasim Hayati-Roodbari, hayati@iau.ac.ir
Received 29 September 2025; Revised from 19 December 2025; Accepted 20 December 2025

Citation: Fazlali A, Hayati-Roodbari N, Kaka GR, Parivar K, Kamalinejad M. Effect of umbilical cord mesenchymal stem cells and *Cichorium intybus* L. root extract on sciatic nerve regeneration. Physiology and Pharmacology 2026; 30: 199-209. http://dx.doi.org/10.22034/phypha.30.2.199

Introduction

The peripheral nervous system (PNS) can regenerate after injury, but the central nervous system (CNS) generally cannot due to specific glial inhibitors. Nerve regeneration depends on both local and systemic factors (Bain JR 1989; Başaran U 2021). Schwann cells, the primary glia in the PNS, promote axonal regrowth and guide axons to their targets (Dabbagh Moghadam F 2020). In unmyelinated axons, Schwann cells offer minimal protection, whereas in myelinated axons, they create the myelin sheath. Each Schwann cell myelinates a single axon segment in the PNS; oligodendrocytes fulfill this role in the CNS (Dabbagh Moghaddam F 2021). The peripheral nerve regenerative environment involves Schwann cells, fibroblasts, collagen, and phagocytes. Post-injury, Schwann cells reactivate development-related genes, mimicking early nerve growth. Both embryonic and adult stem cells self-renew and differentiate, supporting the tissue repair (Bain JR 1989; Başaran U 2021).

Following peripheral nerve injury, Wallerian degeneration (the breakdown of the part of the nerve fiber distal to an injury) leads to the breakdown of the distal axon at the lesion site. Schwann cells are among the first responders, releasing inflammatory cytokines (signaling proteins) such as TNF (tumor necrosis factor), IL-1α, and IL-1β (types of interleukins) within hours of damage (DeLeonibus A 2021). These signals induce the expression of additional mediators like IL-6 (interleukin-6), GM-CSF (granulocyte-macrophage colony-stimulating factor), and IL-10 in Schwann cells and fibroblasts. Chemokines (proteins that attract immune cells), including MCP-1 (monocyte chemoattractant protein-1) and MIP-1α (macrophage inflammatory protein-1 alpha), peak on the first day post-injury, promoting macrophage infiltration at the lesion site. Nerve repair involves regeneration of nerve tissues and associated components, including neurons, glia, myelin, and synapses (Başaran U 2021; Derakhshandeh K 2016). Compared with the CNS, this process is faster and has greater regenerative capacity in the PNS (Derakhshandeh K 2016).

Differentiated Schwann cells repair nerves by replenishing damaged tissue and guiding axonal regrowth via Büngner bands. Bone marrow–derived stem cells show potential for neural repair, but present challenges such as invasiveness and age-related decline (Gu D 2024).

Recent advances in cell isolation have made umbilical cord-derived mesenchymal stem cells (MSCs) an attractive therapeutic option. These cells often express neuronal markers, lack MHC class II, and help minimize immune rejection. Landmark evidence from seminal trials has demonstrated their superior capacity for neuroregeneration when compared to adult stem cells, making them an ethical, readily available, and scalable source for therapy. Further research is required for optimal recovery. The rat sciatic nerve model is preferred due to its reproducibility, physiological similarity to humans, and suitability for controlled lesions (Gu D 2024; T. 2016). Nanotechnology and natural compounds are also being evaluated for nerve regeneration (Hellman et al., 2021).

Cichorium intybus L., a perennial in the Asteraceae family, exhibits multiple bioactivities, including antibacterial, anti-inflammatory, antioxidant, hepatoprotective, anti-tumor, lipid-lowering, and hypoglycemic effects. These effects derive from phytochemicals such as alkaloids, phenolic acids, terpenes, lactones, aliphatic compounds, flavonoids, and polysaccharides (Hosseinzadeh Aghdam V 2016; Huang et al., 2023; Jin et al., 2023; Jung et al., 2016). This study prepared root extracts of *Cichorium intybus L.* and established a rapid, standardized, validated HPTLC protocol for quantifying its phenolics, flavonoids, and triterpenoids, enabling robust separation and measurement. Esculin, a phenolic glycoside, was also standardized and validated by HPTLC (Kamboj and Saluja 2017).

High-performance thin-layer chromatography (HPTLC) is valued for its accuracy, affordability, and sensitivity. It effectively analyzes complex mixtures because it is fast, cost-efficient, and requires minimal sample preparation. HPTLC conserves time and resources, making it ideal for herbal product quality control. With advanced data processing and enhanced techniques, HPTLC delivers results comparable to HPLC and GC, combining efficiency with reliable compound identification (Korshunova and Martynov 2024).

Biodegradable copolymers like polylactide-glycolic acid–polyethylene glycol (PLGA-PEG) serve as scaffolds for cell growth and drug delivery in tissue engineering. PLGA is favored in regenerative medicine for its safety, controllable breakdown rate, and elimination as carbon dioxide and water (Lee et al., 2020).

This study evaluated the combined use of advance current approaches, this study evaluated the combined use of umbilical cord–derived cells cultured on nano-

structured PLGA scaffolds and *Cichorium intybus* L. extract for repairing transected sciatic nerves in male Wistar rats.

Materials and Methods

Materials

The following sections describe the materials, methods, and experimental design employed in this investigation. The following reagents and chemicals were used in this study: Ketamine 10% (Ver Agro, Cat. No. NDC 42023-138-10), Xylazine 2% (Bioveta, Cat. No. NDC 59399-111-50), α-MEM (Inoclon, 13-013), Goat serum (Biowest, Cat. No. S00000S2000/S2000-500), Trypsin-EDTA 10× (Biowest, Cat. No. S00000X0930/X0930-10), Hematoxylin (Padtanteb, Cat. No. 20722), Eosin (Padtanteb, Cat. No. 21658), Xylenol-3,4 (Iran Camex, Cat. No. 106-42-3), Ethanol (Padtanteb, Cat. No. 31258), Phosphate-buffered saline (PBS, Biowest, Cat. No. S00000L0615/L0615-500), Hydrogen peroxide (Sadrashimi, Cat. No. 71930), BrDU (Abcam, Cat. No. AB125306), Dulbecco's Modified Eagle Medium (DMEM, ATCC, Cat. No. 20110-2209), Fetal bovine serum (FBS, Sigma, Cat. No. F7524), Myelin basic protein (MBP) monoclonal antibody (Alexa, USA, Cat. No. sc-271524), Biotin–avidin–HRP secondary antibody (NovaRED, Cat. No. MP-7500), 3,3′-Diaminobenzidine tetrahydrochloride dihydrate (DAB, Acros Organics, Cat. No. 91-95-2), Streptomycin–penicillin (Gibco, Cat. No. 15140122), Dimethylformamide (DMF, Sigma, Cat. No. 68-12-22), Dissection balanced salt solution (DBSS, Sigma), Hank's balanced salt solution (HBSS, Sigma, Cat. No. H1641), and Collagenase enzyme (Sigma, Cat. No. 9001-12-1).

Extraction of the Cichorium Intybus L.

Roots of *Cichorium intybus* L. were harvested from the Rasht region of Guilan Province in August 2022. Botanical authentication was carried out by the Medicinal Plants Herbarium, School of Pharmacy, Shahid Beheshti University of Medical Sciences, Tehran, Iran (Voucher No. SBMU 8311). For extraction, 100 g of shade-dried, coarsely powdered roots were placed into a Soxhlet apparatus with 800 mL of ethanol (96%) and 200 mL of distilled water. The hydroalcoholic extract was concentrated, and residual solvent was removed using a rotary evaporator (Manto et al., 2022).

Determination of Phenolic and Flavonoid Compounds

Phenolic and flavonoid constituents of chicory were identified using high-performance thin-layer chromatography (HPTLC was employed to separate and detect small amounts of chemical substances). HPTLC is recognized for its sensitivity, reproducibility, and simplicity, enabling separation and quantification of compounds at low concentrations. The principle of the method involves two immiscible phases—stationary (a solid layer) and mobile (a solvent)—interacting with analytes (substances being measured) to achieve separation into distinct bands (Moattari et al., 2018).

A 0.2 g sample of the extract was dissolved in 1 mL of ethanol, homogenized, and centrifuged. Five microliters of the supernatant were spotted on TLC plates, which were developed using the following mobile phase:

Ethyl acetate: 10

Formic acid: 1.1

Acetic acid: 1.1

Water: 2.6

Natural product reagents were applied for derivatization, and phenolic and flavonoid compounds were visualized as green or blue spots (Moattari et al., 2018).

Fabrication of PLGA Scaffolds

Electrospinning produced nanofibrous PLGA scaffolds from a PLGA solution in dimethylformamide and chloroform. This solution was loaded into a 5 mL syringe (needle diameter: 0.4 mm), and a 20 kV electric field was applied. The polymer was deposited at 1 mL/h onto grounded foil, creating nanofibrous scaffolds (Moghaddam et al., 2016).

Isolation of Umbilical Cord Stromal Stem Cells

Umbilical cords were washed in dissection-balanced salt solution and sterilized with 70% ethanol for 30 s. Under sterile conditions, cords were rinsed with physiological saline, cut into 3 mm sections, and placed in Hank's balanced salt solution. The surrounding epithelium and vessels were carefully removed, and Wharton's jelly fragments were dissected into small pieces. Tissue was digested with collagenase enzyme (2 μL), and cells were gently pipetted and transferred into culture flasks (Moghaddam et al., 2020).

Culture of Umbilical Cord Stromal Stem Cells

Isolated cells were seeded in T-25 flasks containing DMEM supplemented with L-glutamine, sodium bicar-

bonate, 1% penicillin/streptomycin, and 10% FBS. Cultures were incubated at 37°C with 5% CO_2 in a humidified environment.

Experimental Animals

Forty-five adult male Wistar rats (200–250 g) were obtained from the Pasteur Institute, Tehran, Iran. All experimental procedures were approved by the Ethics Committee of Baghiyatallah University of Medical Sciences (Ethics code: IR.IAU.SRB.REC.1396.893). Animals were housed under controlled conditions (12/12 h light/dark cycle, 23 °C, 55% humidity).

Study Design and Treatment Groups

After a 7-day acclimatization period, rats were randomly divided into nine groups (n = 5 per group) and treated for 8 weeks:

Group 1 (HC): Healthy controls, no treatment.

Group 2 (SNI): Sciatic nerve injury without treatment.

Group 3 (UCCs): SNI + umbilical cord cells (0.5 mL α-MEM containing 1×10^5 UCCs).

Group 4 (CI): SNI + *C. intybus* extract (125 mg/kg/day, i.p.).

Group 5 (CI+UCCs): SNI + *C. intybus* + UCCs.

Group 6 (CI+PLGA/S): SNI + *C. intybus* + PLGA scaffold.

Group 7 (PLGA/S): SNI + PLGA scaffold.

Group 8 (PLGA/S+UCCs): SNI + PLGA scaffold + UCCs.

Group 9 (CI+PLGA/S+UCCs): SNI + *C. intybus* + PLGA scaffold + UCCs.

Surgical Procedures

Sciatic nerve injury was induced under anesthesia with intraperitoneal ketamine (80 mg/kg) and xylazine (5 mg/kg). The right hind limb was shaved, and a 3 cm longitudinal incision was made on the posterolateral thigh to expose the sciatic nerve.

Electrophysiological Assessment

At week 8, electrophysiological measurements were performed under ketamine/xylazine anesthesia. Body temperature was maintained at ~30°C using a heating lamp. Following re-exposure of the sciatic nerve, electromyography was conducted according to previously published protocols (Nikhal and Dambe 2010).

Sciatic Functional Index (SFI)

Two and eight weeks post-surgery, footprints were recorded by applying ink to the hind paws and allowing rats to walk along a 20 × 7 × 60 cm corridor lined with white paper. The sciatic functional index was calculated using the Bain et al. (1989) formula, comparing the operated to the contralateral intact limb (Papetti et al., 2013; Qian et al., 2022).

where EPL = experimental print length, NPL = normal print length, ETS = experimental toe spread, NTS = normal toe spread, EIT = experimental intermediary toe spread, and NIT = normal intermediary toe spread.

Histopathological Examination

At the end of the eighth week, all animals were sacrificed for histological evaluation. Sciatic nerves were dissected and fixed in 10% neutral-buffered formalin for 24 h. Following fixation, tissues were washed in running tap water for 4–8 h, dehydrated through a graded ethanol series (50–100%), and cleared with xylene. The samples were then embedded in paraffin, sectioned at 5 µm thickness, and stained with hematoxylin and eosin (H&E). Sections were examined using a conventional light microscope (Rasmussen et al., 2014).

Statistical Analysis

Morphometric measurements including nerve diameter, vessel diameter, and vessel number were obtained using Motic Image 2000 software (Release 1.2). Data were expressed as mean ± SD, and statistical analyses were performed using GraphPad Prism (v.8). Differences between groups were evaluated by one-way ANOVA followed by Tukey's post hoc test. A p-value < 0.05 was considered statistically significant (Rekler and Kalcheim 2021).

Results

Nerve Conduction Velocity (NCV)

NCV (m/s) was significantly reducedin all treatment groups (UCCs, CI, CI+UCCs, CI+PLGA/S, PLGA/S, PLGA/S+UCCs, and CI+PLGA/S+UCCs) compared with the healthy control (HC, $p<0.0001$), but remained significantly higher compared with the sciatic nerve injury (SNI) group ($p<0.0001$). A faster NCV, as observed in the CI+PLGA/S+UCCs group, suggests more efficient nerve impulse transmission, which is critical for regaining muscle coordination and movement. Notably,

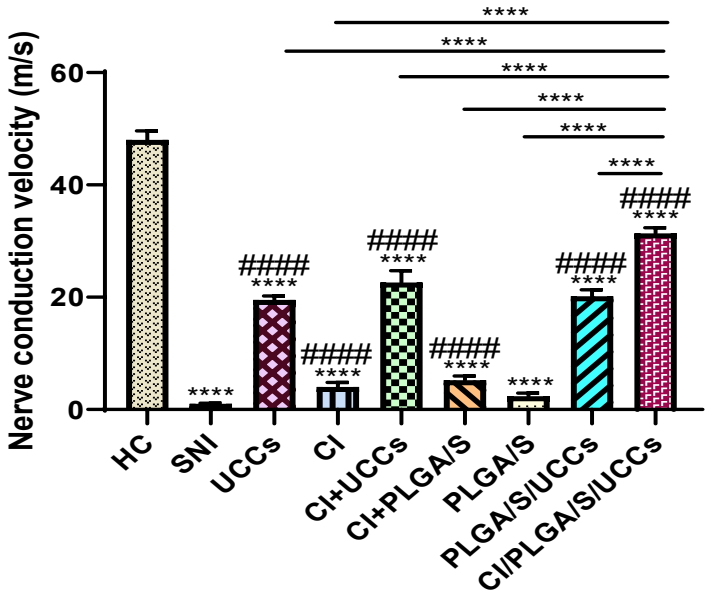

FIGURE 1. NCV rate (m/s) in HC, SNI, UCCs, CI, CI+UCCs, CI+PLGA/S, PLGA/S, PLGA/S/UCCs, and CI/PLGA/S/UCCs groups. Comparison of treated groups with HC ****P<0.0001; Comparison of groups treated with SNI ####P<0.0001.

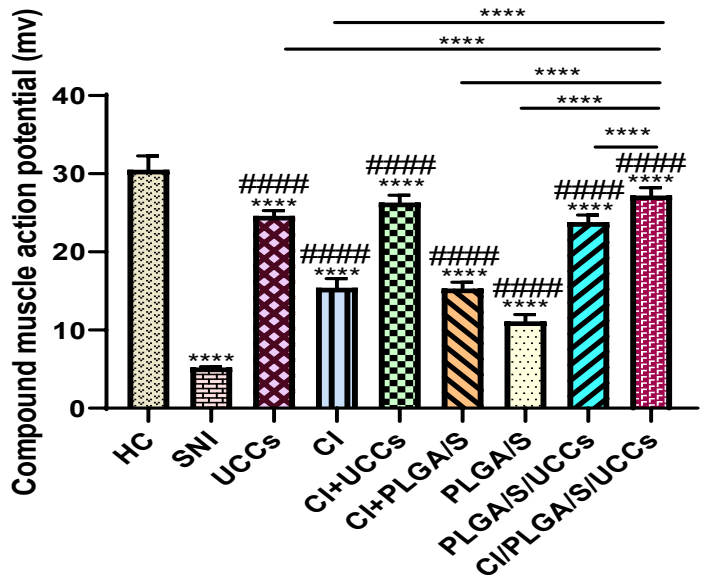

FIGURE 2. Electrophysiological examination was performed for HC, SNI, UCCs, CI, CI+UCCs, CI+PLGA/S, PLGA/S, PLGA/S/UCCs, and CI/PLGA/S/UCCs groups. Comparison of treated groups with HC ****P<0.0001; Comparison of groups treated with SNI ####P<0.0001.

NCV in the CI+PLGA/S+UCCs group was markedly faster than in all other treatment groups after 8 weeks ($p<0.001$), indicating synergistic benefits of the combined therapy for axonal regeneration (Figure 1).

Electrophysiological Examination

Compound muscle action potential (CMAP, mV) was significantly reduced in all treatment groups relative to HC ($p<0.0001$) but increased compared with SNI ($p<0.0001$). The CI+PLGA/S+UCCs group demonstrated the greatest improvement, with significantly higher CMAP values compared with all other treatment groups ($p<0.001$) (Figure 2).

Histomorphometric Analysis

Nerve fiber density decreased in all treated groups

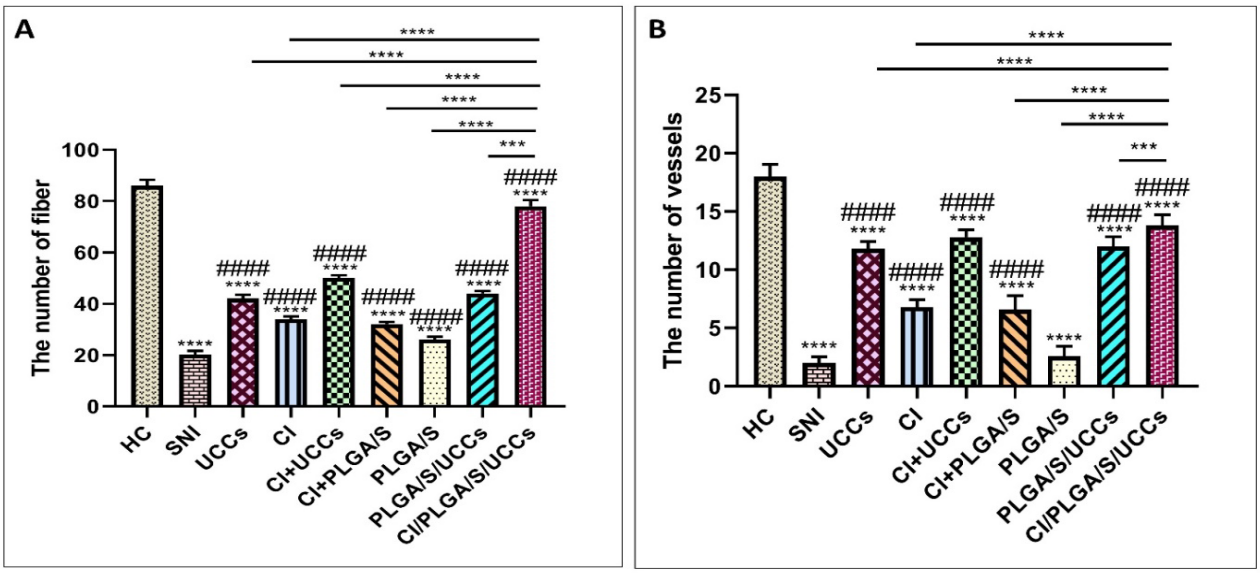

FIGURE 3. The number of fiber (A) and vessels in HC, SNI, UCCs, CI, CI+UCCs, CI+PLGA/S, PLGA/S, PLGA/S/UCCs, and CI/PLGA/S/UCCs groups after 8 weeks. Comparison of treated groups with HC ****P<0.0001; Comparison of groups treated with SNI ####P<0.0001.

compared to HC (p<0.0001) but was significantly higher than in the SNI group (p<0.0001). After 8 weeks, fiber counts in the CI+PLGA/S+UCCs group exceeded those of UCCs, CI, CI+UCCs, CI+PLGA/S, PLGA/S, and PLGA/S+UCCs groups (all p<0.0001; PLGA/S+UCCs p<0.001) (Figure 3A).

Similarly, vessel density was significantly reduced in all groups relative to HC (p<0.0001) but elevated compared with SNI (p<0.0001). The CI+PLGA/S+UCCs group exhibited the highest number of vessels among all treated groups (p<0.0001 vs. UCCs, CI, CI+PLGA/S, PLGA/S; p<0.001 vs. PLGA/S+UCCs) (Figure 3B).

Fiber, Axon, Vessel, and Myelin Area

Quantitative analysis of the largest cross-sectional areas of fibers, axons, vessels, and myelin (μm²) revealed significant increases in the CI+PLGA/S+UCCs group compared with all other treatment groups (p<0.0001) (Figure 4A–D).

SFI Results

The footprints of the HC, SFI, PLGA, CI, UCCs, CI+UCCs, CI+PLGA, PLGA+UCCs, and CI+PLGA+UCCs groups were reported in Figure 5A. The mean of the SFI rate in animals after surgery was significantly decreased and tended to -100. Two (Figure 5B) and 8 (Figure 5C) weeks after surgery, the SFI mean was assessed in both control and treatment groups. The results of SFI showed that the UCCs, CI, CI+UCCs, CI+PLGA/S, PLGA/S, PLGA/S/UCCs, and CI/PLGA/S/UCCs groups had a significant increase compared to the HC group (P<0.0001). Conversely, the UCCs, CI, CI+UCCs, CI+PLGA/S, PLGA/S, PLGA/S/UCCs, and CI/PLGA/S/UCCs groups exhibited a significant decrease compared to the SNI group (p<0.0001). The CI/PLGA/S/UCCs treatment group had a lower SFI compared to the UCCs, CI, CI+UCCs, CI+PLGA/S, PLGA/S, and PLGA/S/UCCs (p<0.0001).

Analysis Method: High-Performance Thin-Layer Chromatography

The use of *Cichorium intybus* L. extract in this study is due to its anti-inflammatory effects, which aid in the healing of sciatic nerve injury. The anti-inflammatory effect of *Cichorium intybus* L. is attributed to the presence of phenolic and flavonoid compounds. Using HPTLC, phenolic and flavonoid compounds are separated and determined.

To identify phenolic and flavonoid compounds in *Cichorium intybus* L., derivatization (staining) was performed (Figure 6, A-F).

Discussion

This in vivo study evaluated the effects of umbilical

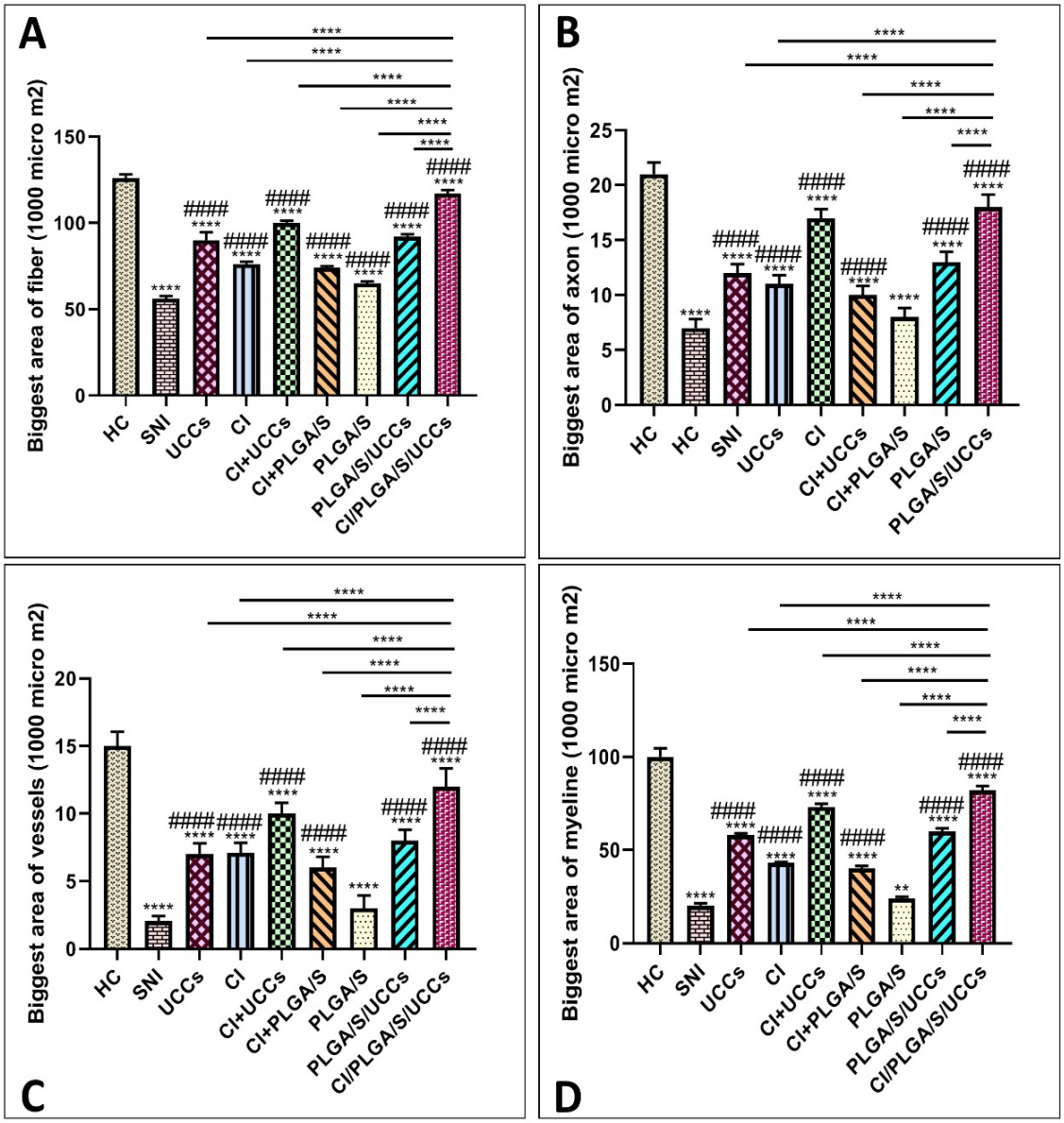

FIGURE 4. Biggest area of fiber (A), axon (B), vessels (C) and myeline (D) (1000 micro m2) in HC, SNI, UCCs, CI, CI+UCCs, CI+PLGA/S, PLGA/S, PLGA/S/UCCs, and CI/PLGA/S/UCCs groups after 8 weeks. Comparison of treated groups with HC **P<0.01, ****P<0.0001; Comparison of groups treated with SNI ####P<0.0001.

cord-derived cells (UCCs) in combination with PLGA scaffolds and *Cichorium intybus* L. extract on sciatic nerve regeneration. The assessment encompassed behavioral, electrophysiological, and histological parameters. Looking ahead, translating this tri-modal therapy from rat models to human clinical applications will involve addressing several key steps. Initial first-in-human trials could focus on assessing safety and dosage, likely requiring close collaboration with regulatory bodies such as the FDA to ensure compliance with current guidelines. Overcoming these regulatory hurdles is essential to bridge the gap between successful animal studies and potential therapeutic use in humans.

The SFI test is a widely accepted method for assessing functional recovery following sciatic nerve injury. Previous studies have shown that pharmacological interventions such as dexamethasone (Rekler and Kalcheim 2021) or ulinastatin (Saini et al., 2014) significantly enhance nerve regeneration. Consistent with these findings, the CI+PLGA/S+UCCs group demonstrated superior recovery across functional, electrophysiological, and histological parameters.

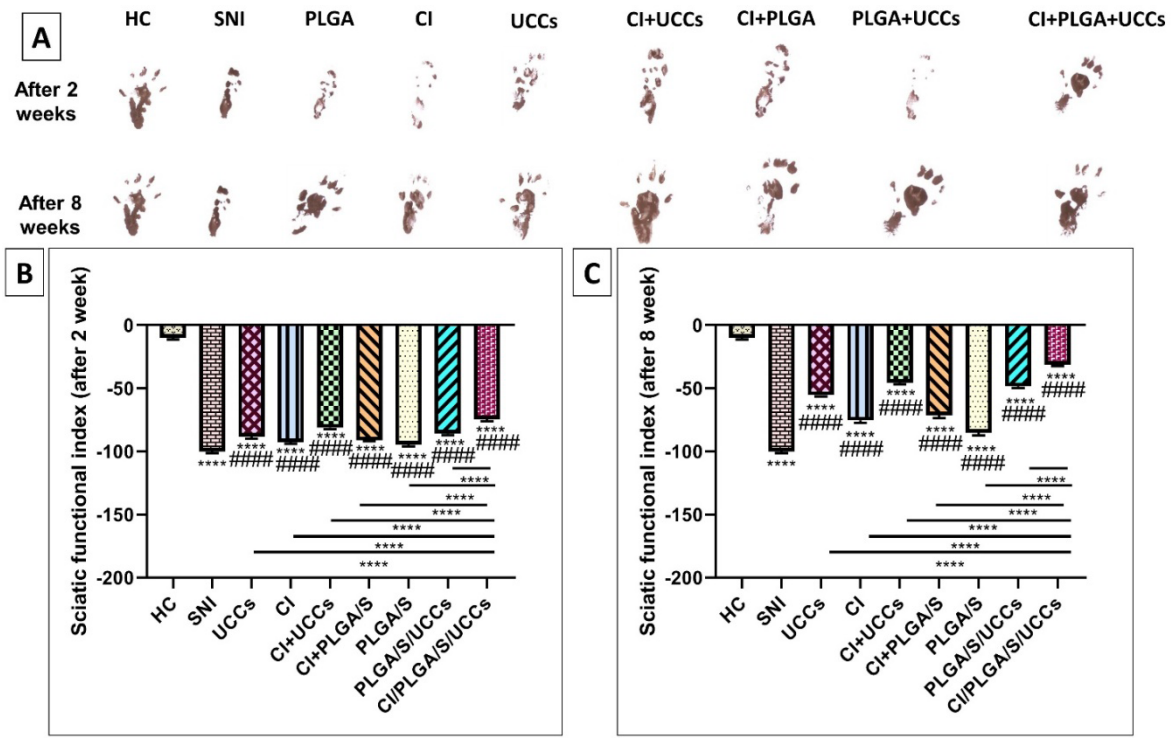

FIGURE 5. Footprints change at 2 and 8 weeks after surgery (A). Comparison of the SFI index functional recovery in HC, SNI, UCCs, CI, CI+UCCs, CI+PLGA/S, PLGA/S, PLGA/S/UCCs, and CI/PLGA/S/UCCs groups after 2 (B) and 8 (C) weeks. Comparison of treated groups with HC ****P<0.0001; Comparison of groups treated with SNI ####P<0.0001.

Peripheral nerve injury triggers degenerative mechanisms such as inflammatory cytokine release, fibroblast activation, and collagen deposition, which can impair regeneration if the microenvironment is uncontrolled (Salama et al., 2016; Sishu and Selvaraj 2024; Soluki et al., 2022). Inflammation leads to macrophage and neutrophil infiltration, myelin debris clearance, and remyelination by Schwann cells (Starhof et al., 2018). The anti-inflammatory and antioxidant properties of C. intybus, attributed to flavonoids and triterpenes (Tuğ Kılkış et al., 2015; Vest et al., 2020), likely improved regeneration by modulating this environment.

These results are consistent with studies demonstrating that biomaterials such as PLGA, when combined with neurotrophic or anti-inflammatory agents, enhance nerve regeneration. For example, erythropoietin-PLGA-PEG scaffolds have increased vascular density and myelination after sciatic nerve injury, while laminin–chitosan–PLGA conduits with Schwann cells facilitated the regeneration of thick, well-myelinated axons (Wong et al., 2019; Zahoor et al., 2022; Zhang et al., 2020).

PLGA scaffolds combined with *C. intybus* extract and UCCs provide a favorable environment for nerve regeneration, angiogenesis, and remyelination. Though PLGA scaffolds are biocompatible and biodegradable, contamination during surgery can cause inflammation. *C. intybus* extract reduces this risk through anti-inflammatory properties and supports nerve cell viability by limiting Wallerian degeneration. A mechanistic hypothesis suggests that the porous structure of PLGA scaffolds could facilitate the gradual release of C. intybus extract, prolonging its therapeutic action. As a result, this controlled release and sustained activity may enhance the anti-inflammatory effects and support continuous neural repair processes, thereby strengthening the observed synergy.

Conclusion

Peripheral nerve injuries are common and can result in severe health complications, financial burdens, and permanent functional loss. This study demonstrated that combining umbilical cord-derived cells, PLGA scaffolds, and *Cichorium intybus* L. extract accelerated sciatic nerve repair in rats. This combination enhanced nerve regeneration, myelination, and recovery, suggesting potential as an effective option for peripheral nerve

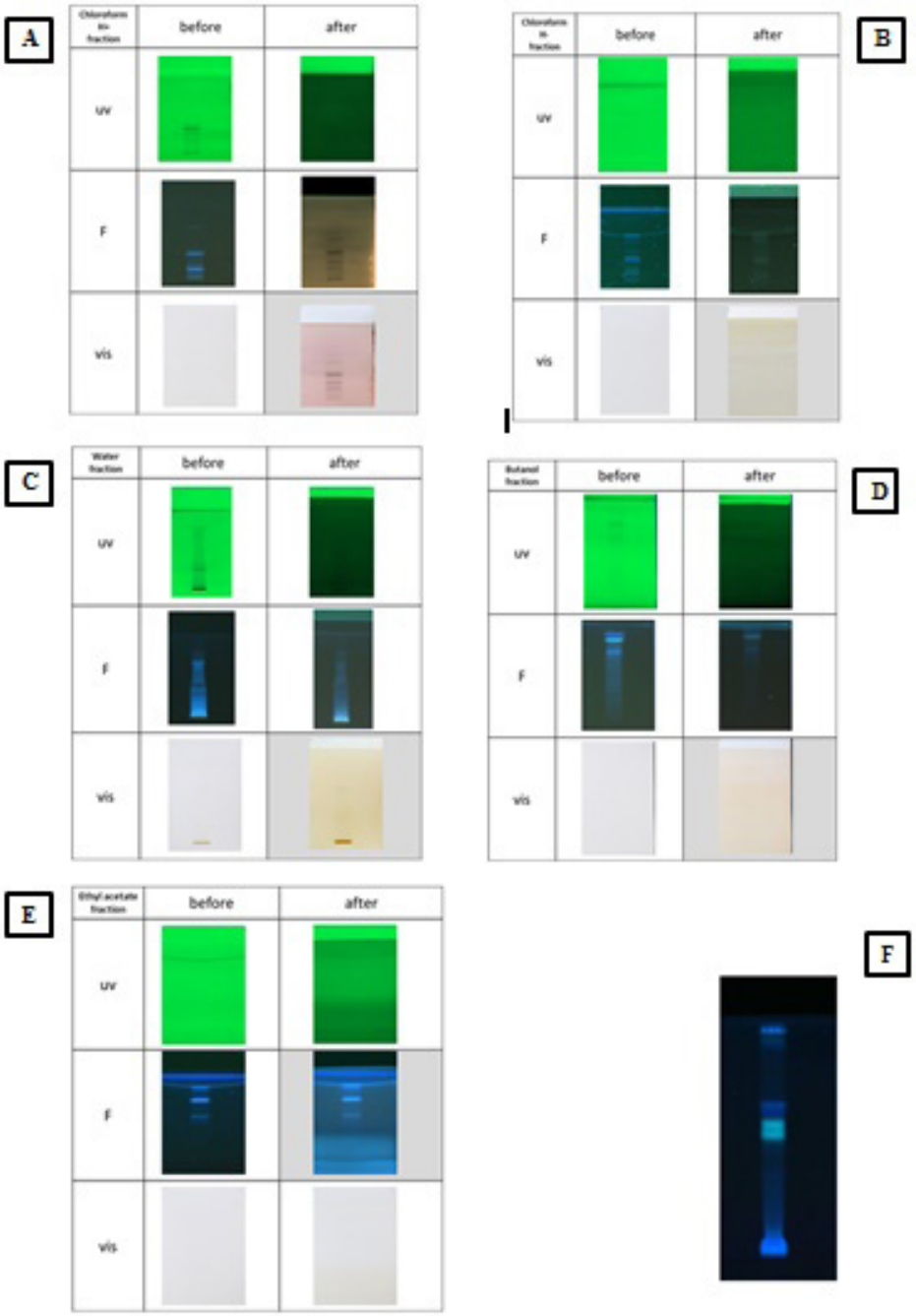

FIGURE 6. A) Analysis Method: High Performance Thin Layer Chromatography Chloroform extraction (terpenes, strolls) Stationary Phase: Sillica geL 60 F 254 HPTLC Plate 5*10 Mobile Phase: Hexane-Ethyl acetate -Ethanol-Formic acid (8-2-1-1) Derivatization: AnisAldehyde -H2S04.
B) Analysis Method: High Performance Thin Layer Chromatography. Chloroform extraction (Nitrogen compounds) Stationary Phase: Sillica geL 60 F 254 HPTLC Plate 5*10 Mobile Phase: Chloroform- Methanol Diethyl Amine 8-0.5-0.5 Derivatization Dragendorff's.
C) Analysis Method: High Performance Thin Layer Chromatography Ethyl acetate extraction (flavonoids, phenolics) Stationary Phase: Sillica geL 60 F254 HPTLC Plate 5*10 Mobile Phase: Toluene - Acetone-Formic acid 4-4-1 Derivatization: natural products.
D) Analysis Method: High Performance Thin Layer Chromatography Butanol extraction (saponins) Stationary Phase: Sillica geL 60 F 254 HPTLC Plate 5*10 Mobile Phase: Chloroform-Acetic acid-Methanol-water 5-4-1-1 Derivatization: FeC13.
E) Analysis Method: High Performance Thin Layer Chromatography water extraction (tannins....) Stationary Phase: Sillica gel 60 F 254 HPTLC Plate 10*10 Mobile Phase: Ethyl acetate-Butanol-Methanol- Acetic Acid -water (3-2-1-1-1) Derivatization: Metanol-H2SO4 (10%).
F) A green and blue colored spot indicates the presence of phenolic and flavonoid compounds in chicory extract.

repair. However, it is important to note some limitations. The optimal dosing and long-term safety of this treatment remain uncertain, necessitating further research. Additionally, scaling this approach for clinical application presents challenges that warrant exploration. Addressing these unanswered questions will be crucial for future developments.

Statement on Manuscript Originality and Editing

Plagiarism detection tools were employed to identify and address overlapping text, ensuring the manuscript's originality and scientific accuracy. Manual editing was conducted to improve clarity, logical flow, and adherence to academic standards.

References

Bain JR M S, Hunter D A. Functional evaluation of complete sciatic, peroneal, and posterior tibial nerve lesions in the rat. Plastic and Reconstructive Surgery 1989; 83: 129-136. https://doi.org/10.1097/00006534-198901000-00024

Başaran U G E, Yaman C, Çopur Doğrusöz M, Mut H. Antioxidants and mineral contents of chicory as coffee additive. Turkish Journal of Agriculture - Food Science and Technology 2021; 9: 217-223. https://doi.org/10.24925/turjaf.v9i1.217-223.3859

Dabbagh Moghadam F H S, Mortazavi P, Nabiouni M, Hayati Roodbari N. Evaluation of the effect of Melittin on liver and renal biochemical markers and KI67 expression in mice with experimentally-induced breast cancer. Journal of Comparative Pathology 2020; 17: 3045-3058.

Dabbagh Moghaddam F A I, Marzbankia E, Farid M, Khaledi L, Reihani AH. Delivery of melittin-loaded niosomes for breast cancer treatment: an in vitro and in vivo evaluation of anti-cancer effect. Cancer Nanotechnol 2021; 12. https://doi.org/10.1186/s12645-021-00085-9

DeLeonibus A R M, Fahradyan V, Silver J, Rampazzo A, Bassiri Gharb B. A meta-analysis of functional outcomes in rat sciatic nerve injury models. Microsurgery 2021; 28: 295-286. https://doi.org/10.1002/micr.30713

Derakhshandeh K K M, Hemati Azandaryani A, Bahrami G, Ghanbari K. Pharmacokinetic study of furosemide incorporated PLGA microspheres after oral administration to rat. Iranian Journal of Basic Medical Sciences 2016; 19: 1055-1049.

Gu D X Y, Ding Z, Qian J, Gu X, Bai H,. Inflammation in the Peripheral Nervous System after Injury. Biomedicines 2024; 5: 1256. https://doi.org/10.3390/biomedicines12061256

Hellman A, Clum A, Maietta T, Srikanthan A, Patel V, Panse D, et al. Effects of external low intensity focused ultrasound on inflammatory markers in neuropathic pain. Neuroscience Letters 2021; 757: 135977. https://doi.org/10.1016/j.neulet.2021.135977

Hosseinzadeh Aghdam V M N. High performance thin layer chromatography. Journal of Iran Laboratory Knowledge 2016; 4.

Huang W, Yi S, Zhao L. Genetic features of young and aged animals after peripheral nerve injury: implications for diminished regeneration capacity. Cellular and Molecular Neurobiology 2023; 43: 4363-4375. https://doi.org/10.1007/s10571-023-01431-8

Jin M Y, Weaver T E, Farris A, Gupta M, Abd-Elsayed A. Neuromodulation for peripheral nerve regeneration: systematic review of mechanisms and in vivo highlights. Biomedicines 2023; 11: 1145. https://doi.org/10.3390/biomedicines11041145

Jung N, Park S, Choi Y, Park J-W, Hong Y B, Park H H C, et al. Tonsil-derived mesenchymal stem cells differentiate into a schwann cell phenotype and promote peripheral nerve regeneration. International Journal of Molecular Sciences 2016; 17: 1867. https://doi.org/10.3390/ijms17111867

Kamboj A, Saluja A K. Development of validated HPTLC method for quantification of stigmasterol from leaf and stem of Bryophyllum pinnatum. Arabian journal of Chemistry 2017; 10: 2644-2650. https://doi.org/10.1016/j.arabjc.2013.10.006

Korshunova T, Martynov A. The phyloperiodic approach removes the "cryptic species" and puts forward multilevel organismal diversity. Diversity 2024; 16: 220. https://doi.org/10.3390/d16040220

Lee J I, Hur J M, You J, Lee D H. Functional recovery with histomorphometric analysis of nerves and muscles after combination treatment with erythropoietin and dexamethasone in acute peripheral nerve injury. PLoS One 2020; 15: e0238208. https://doi.org/10.1371/journal.pone.0238208

Manto K M, Govindappa P K, Martinazzi B, Han A, Hegarty J P, Koroneos Z, et al. Erythropoietin-PLGA-PEG as a local treatment to promote functional recovery and neurovascular regeneration after peripheral nerve injury. Journal of Nanobiotechnology 2022; 20: 461. https://doi.org/10.1186/s12951-022-01666-5

Moattari M, Kouchesfehani H M, Kaka G, Sadraie S H, Naghdi M, Mansouri K. Chitosan-film associated with mesenchymal stem cells enhanced regeneration of peripheral nerves: A rat sciatic nerve model. Journal of Chemical

Neuroanatomy 2018; 88: 46-54. https://doi.org/10.1016/j.jchemneu.2017.10.003

Moghaddam F D, Hamedi S, Dezfulian M. Anti-tumor effect of C-phycocyanin from Anabaena sp. ISC55 in inbred BALB/c mice injected with 4T1 breast cancer cell. Comparative Clinical Pathology 2016; 25: 947-952. https://doi.org/10.1007/s00580-016-2285-2

Moghaddam F D, Mortazavi P, Hamedi S, Nabiuni M, Roodbari N H. Apoptotic effects of melittin on 4T1 breast cancer cell line is associated with up regulation of Mfn1 and Drp1 mRNA expression. Anti-Cancer Agents in Medicinal Chemistry 2020; 20: 790-799. https://doi.org/10.2174/1871520620666200211091451

Nikhal S, Dambe P. Hydroalcoholic extraction of Mangifera indica (leaves) by soxhletion. International Journal of Pharmaceutical Sciences and Research 2010: 78-81.

Papetti A, Mascherpa D, Carazzone C, Stauder M, Spratt D A, Wilson M, et al. Identification of organic acids in Cichorium intybus inhibiting virulence-related properties of oral pathogenic bacteria. Food Chemistry 2013; 138: 1706-1712. https://doi.org/10.1016/j.foodchem.2012.10.148

Qian C, Zhang Z, Zhao R, Wang D, Li H. Effect of acellular nerve scaffold containing human umbilical cord-derived mesenchymal stem cells on nerve repair and regeneration in rats with sciatic nerve defect. Annals of Translational Medicine 2022; 10: 483. https://doi.org/10.21037/atm-22-1578

Rasmussen M K, Klausen C L, Ekstrand B. Regulation of cytochrome P450 mRNA expression in primary porcine hepatocytes by selected secondary plant metabolites from chicory (Cichorium intybus L.). Food Chemistry 2014; 146: 255-263. https://doi.org/10.1016/j.foodchem.2013.09.068

Rekler D, Kalcheim C. From neural crest to definitive roof plate: the dynamic behavior of the dorsal neural tube. International Journal of Molecular Sciences 2021; 22: 3911. https://doi.org/10.3390/ijms22083911

Saini M, Khani A, Bala M, Abding M, Farooqi H. Development of a validated HPTLC method for quantification of Esculin in different fractions of Cichorium intybus leaf extract. International Journal of Pharmacy and Pharmaceutical Sciences 2014; 6: 278-282.

Salama A H, Mahmoud A A, Kamel R. A novel method for preparing surface-modified fluocinolone acetonide loaded PLGA nanoparticles for ocular use: in vitro and in vivo evaluations. AAPS PharmSciTech 2016; 17: 1159-1172. https://doi.org/10.1208/s12249-015-0448-0

Sishu N K, Selvaraj C I. Phytochemistry, pharmacological applications, and therapeutic effects of green synthesized nanomaterials using Cichorium species-a comprehensive review. Naunyn-Schmiedeberg's Archives of Pharmacology 2024; 397: 8527-8559. https://doi.org/10.1007/s00210-024-03221-5

Soluki M, Mahmoudi F, Abdolmaleki A. Therapeutic factors in ischemic stroke control. The Neuroscience Journal of Shefaye Khatam 2022; 10: 77-91. https://doi.org/10.52547/shefa.10.4.77

Starhof C, Winge K, Heegaard N, Skogstrand K, Friis S, Hejl A. Cerebrospinal fluid pro-inflammatory cytokines differentiate parkinsonian syndromes. Journal of Neuroinflammation 2018; 15: 305. https://doi.org/10.1186/s12974-018-1339-6

T. G. Nerve regeneration in the peripheral and central nervous systems. Journal of Physiology 2016; 1: 3520-3517. https://doi.org/10.1113/JP270898

Tuğ Kılkış B, Er K, Taşdemir T, Yildirim M, Taskesen F, Tümkaya L, et al. Neurotoxicity of various root canal sealers on rat sciatic nerve: an electrophysiologic and histopathologic study. Clinical Oral Investigations 2015; 19: 2091-2100. https://doi.org/10.1007/s00784-015-1447-y

Vest M, Guida A, Colombini C, Cordes K, Pena D, Maki M, et al. Closing the Gap Between Mammalian and Invertebrate Peripheral Nerve Injury: Protocol for a Novel Nerve Repair. JMIR Research Protocols 2020; 9: e18706. https://doi.org/10.2196/18706

Wong Y-R, Pang X, Lim Z Y, Du H, Tay S-C, McGrouther D A. Biomechanical evaluation of peripheral nerves after crush injuries. Heliyon 2019; 5: e01557. https://doi.org/10.1016/j.heliyon.2019.e01557

Zahoor I, Anjum N, Ganaie T A, Allai F M, Al-Ghamdi A A, Abbasi A M, et al. Effect of hybrid drying technique on non-traditional Chicory (Cichorium intybus L.) herb: Phytochemical, antioxidant characteristics, and optimization of process conditions. Frontiers in Sustainable Food Systems 2022; 6: 1002396. https://doi.org/10.3389/fsufs.2022.1002396

Zhang J, Zhang Y, Chen L, Rao Z, Sun Y. Ulinastatin promotes regeneration of peripheral nerves after sciatic nerve injury by targeting let-7 microRNAs and enhancing NGF expression. Drug Design, Development and Therapy 2020: 2695-2705. https://doi.org/10.2147/DDDT.S255158